Morphological Adjustments on Cable-Net Supporting the Reflector Panels of FAST Based on Rotation Axis Matrices and Geodesic Tracing Algorithm

Jie Liang [1, *], Mingzhe Liu [1], Xunyang Wang [2], Peiyu Wang [1]

[1] School of Civil Engineering, Lanzhou University of Technology, Lanzhou, China, 730000

[2] College of Science, Lanzhou University of Technology, Lanzhou, China, 730000

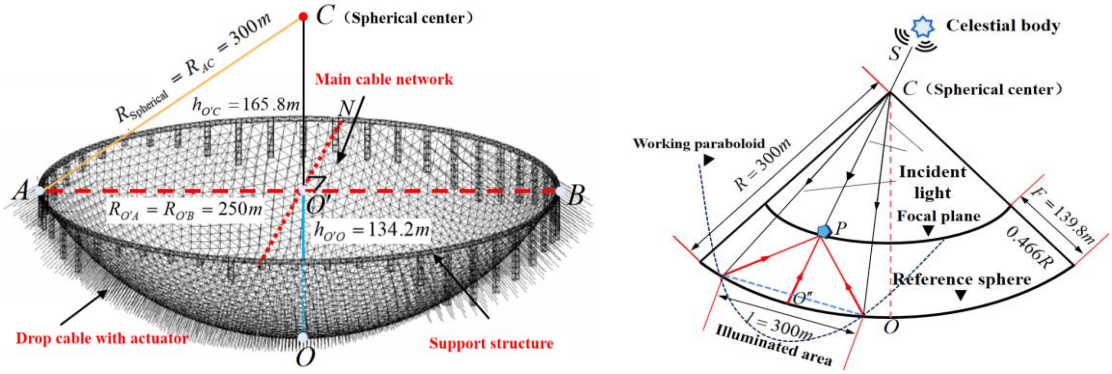
* Corresponding Author Email: lut_lj7364414@163.com

Abstract. The key of FAST active reflection panel cable-net adjustment technology is to regulate the reflection sphere to the working paraboloid. The principle is to realize the position change by stretching the pull-down cable's control node through the actuator. In this paper, based on the rotation axis transformation equation of the working paraboloid in the ground state, combined with the constraint conditions of actuator expansion, the geodesic tracing algorithm was used to map the geodesic nodes of the spatial cable-net quickly and efficiently. Through numerical verification of 2336 cable points from area A-E, the model quickly and stably adjusts the cable-net layout according to different star observation angles, so that the working face approaches to the standard paraboloid, and the optimal layout scheme of the cable-net displacement pulling of the active reflective surface of FAST can be obtained under any observation angle.

Keywords: FAST, Layout of Cable-Net Structure, Rotation Axis Matrices, Geodesic Tracing.

1. Introduction

In 2016, China's Sky Eye (FAST) was successfully built as the world's largest radio telescope in China, its land use marks another major breakthrough in the field of radio astronomy in China [1]. FAST consists of five parts, such as an active reflecting surface, measurement and control system, signal receiving system (feed cabin), etc. The initial configuration of the reflecting surface is spherical and hinged by orthogonal steel cables on intersecting internal nodes [2]. The reflection surfaces and parameters of the overall deformation cable-net are shown in figure 1(a).



(a) (b)

Figure 1. FAST cable-net layout parameters (a) and profile optical path (b)

When the active reflector is not working, it is in the reference state, presenting as a reference sphere with a radius of 300m and a caliber of 500m. During astronomical observation, the position and direction of the reflector panel can be changed by changing the radial expansion of the actuator fixed on the ground end and pulling the connected main cable node. At this time, it is required that the main reflecting surface in the illumination area (effective area of diffuse reflection) with an aperture of 300m forms a paraboloid, so that the incident electromagnetic wave is focused on the feed cabin P on the focal surface. The focal plane formed by the movement trajectory of the receiving plane center

of the feed cabin is concentric with the reference sphere, and the radius difference is $F=0.466R$. See figure 1(b) for the working optical path of FAST's geometric section.

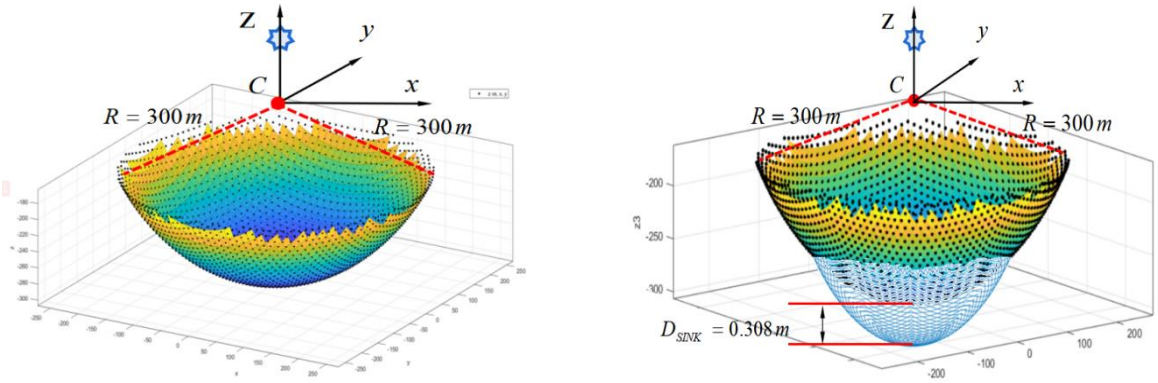
The orientation of the celestial body S is determined by the azimuth and elevation angle. After the reference ideal paraboloid is given, the simulation research objective is to make the reflector as close to the ideal paraboloid as possible by adjusting the control point's cable mesh tension and the actuator and the main reflector when the observed star is located at a specific observation angle.

2. Materials and methods

2.1. Data preprocessing

① Calculate the equations of the reference sphere and the ideal paraboloid:

Data and reference examples are from http://www.mcm.edu.cn/. Coordinates and numbers of all main cable nodes are fitted. When the measured celestial body is located directly above the reference sphere (The working paraboloid at $\alpha=0^{\circ}$ and $\beta=90^{\circ}$), the obtained reference sphere curve and ideal paraboloid are shown in figure 2(a) and 2(b) respectively. The lowest point of the ideal paraboloid is 0.308m lower than that of the sphere.



(a) (b)

Figure 2. The fitting results of the reference sphere (a) and the ideal paraboloid (b)

② Construct the basic coordinate system:

When the measured celestial body S is located directly above the reference sphere ($\alpha=0^{\circ}$, $\beta=90^{\circ}$), the intersection point between the line SC and the reference sphere is set as O, the reference spherical center C is taken as the origin of the coordinate, while the positive directions of x, y and z axes are determined in the direction of $\overrightarrow{O'B}, \overrightarrow{O'N}, \overrightarrow{O'C}$ vector respectively, and the basic space rectangular coordinate system $C-xyz$ is established according to the right-hand rule [3]:

The spherical crown of FAST is located below the z axis as a whole, thus the basic spherical equation can be simultaneously transformed as:

$$z=\sqrt{300^2-x^2-y^2},\quad x,y\in[-250m,250m] \tag{1}$$

The ideal paraboloid is a paraboloid with an upper caliber of 300m and the lowest point of 300.308m from the origin O. The equation of the base paraboloid is derived from its standard equation:

$$x^2+y^2-299.6923(z+300.308)=0 \tag{2}$$

③ FAST spatial domain meshing:

In the process of FAST observation, any area of the spherical cable network will be adjusted to the specified paraboloid, so it is hoped that the mesh division of the spherical cable-net will be more

uniform, and there is no obvious primary and secondary force of the main cable-net [4-6]. At the same time, the fewer types and quantities of spherical mesh, the more conducive to the dynamic adjustment of the reflecting surface structure.

Therefore, number the 2226 cable-net nodes and quintuple the reference sphere of FAST, the central angle about any part is 72°. As shown in figure 3 (due to the geometric inhomogeneity of the reference sphere of FAST, the number of cable points in each region is slightly different), the cable network coordinates in the reference coordinate system are known, and the geodesic method is used to adjust 860 vertices of reflection panels in each partition.

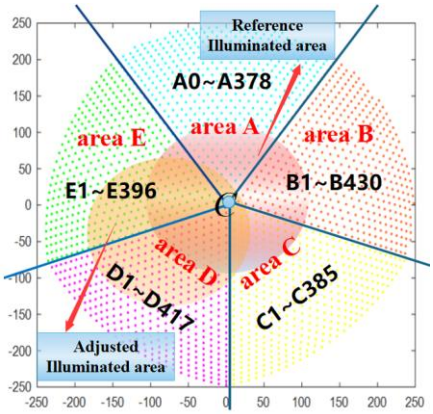


Figure 3. Top view of FAST meshing with main cable-net nodes numbering

2.2. The methods introduction

2.2.1 Rotation axis transformation

When the direction of the celestial body changes, angles α and β are the linear plane angles between SC and the plane Cxy , Cyz respectively. Set the origin unchanged, and use Euler's rotation theorem [7] to transform the rotation axis, making the axis z'' coincide with the line SC after two transpositions. Therefore, the transfer of cable-nets node dots cluster in the illuminated region of the original coordinate system is realized, while the motion law of working parabolic cable network nodes relative to the reference sphere can be described when the incident direction of the star changes.

2.2.2 The geodesic tracing algorithm

In this paper, the algorithm adopts the idea of "turning a curve into a straight one". The problem of the cable-net layout of the working parabolic surface is transformed into a plane search problem. First, find the geodesic lines on the plane projection, and then the geodesic lines on the plane are converted to the original space surface according to the mapping relationship of cable-net nodes.

The basic idea of the algorithms are as follows: after inputting the two specified endpoints of the geodesic to be obtained, a triangular reflector panel projection mesh belt [8] connecting the two endpoints is found on the curved surface. After expanding on the plane, this triangle belt must be traversed by a straight line connecting the two ends of the cable-net. Mapping this line to a working paraboloid is a geodesic. Then, through the radial telescopic restriction conditions of the actuator, the computer simulation is used to force the actuator to pull the inconsistent cable-net move, so that the working paraboloid is as close to the ideal paraboloid as possible.

3. The establishment and solution of the simulation model

3.1. Rotation axis matrices

When the azimuth angle of the star to be measured is $\alpha = 36.795^{\circ}$ and $\beta = 78.169^{\circ}$, the original rectangular coordinate system $C - xyz$ is rotation transformed twice to make the vector $\overrightarrow{SC}$

coincide with the positive direction of the z axis of the $C-x''y''z''$ coordinate system. See figure 4 for the specific coordinate transformation process:

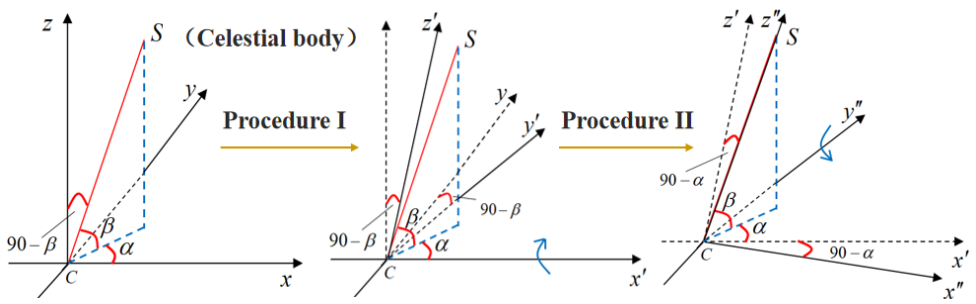


Figure 4. Rotation axis transformation process diagram

Rotation transformation I: Carry out rotation transformation with Cx as the rotation axis of the original coordinate system, rotate the axis z clockwise from right to left with $(90-\beta)°$, and the transition coordinate system after rotation is $C-x'y'z'$. At this time, the rotation matrix is:

$$\Lambda_1=\begin{bmatrix}1 & 0 & 0\\ 0 & \cos\dfrac{(90-\beta)\pi}{180} & \sin\dfrac{(90-\beta)\pi}{180}\\ 0 & -\sin\dfrac{(90-\beta)\pi}{180} & \cos\dfrac{(90-\beta)\pi}{180}\end{bmatrix} \tag{3}$$

Rotation transformation II: Takes Cy' as the rotation axis of the transition coordinate system obtained from the first transformation, and rotate $(90-\alpha)°$ clockwise along the y' axis so that the positive direction of z' axis coincides with the line SC, the final coordinate system is $C-x''y''z''$, and then give the second transformation matrix:

$$\Lambda_2=\begin{bmatrix}\cos\dfrac{(90-\alpha)\pi}{180} & 0 & -\sin\dfrac{(90-\alpha)\pi}{180}\\ 0 & 1 & 0\\ \sin\dfrac{(90-\alpha)\pi}{180} & 0 & \cos\dfrac{(90-\alpha)\pi}{180}\end{bmatrix} \tag{4}$$

According to the continuity principle of Euler rotation transformation, for any stars with observation combination angle of (α,β), the total transformation matrix is:

$$\Lambda_3=\Lambda_1\times\Lambda_2=\begin{bmatrix}1 & 0 & 0\\ 0 & \cos\dfrac{(90-\beta)\pi}{180} & \sin\dfrac{(90-\beta)\pi}{180}\\ 0 & -\sin\dfrac{(90-\beta)\pi}{180} & \dfrac{\cos(90-\beta)\pi}{180}\end{bmatrix}\cdot\begin{bmatrix}\cos\dfrac{(90-\alpha)\pi}{180} & 0 & -\sin\dfrac{(90-\alpha)\pi}{180}\\ 0 & 1 & 0\\ \sin\dfrac{(90-\alpha)\pi}{180} & 0 & \cos\dfrac{(90-\alpha)\pi}{180}\end{bmatrix} \tag{5}$$

The total matrix Λ_3 represents the mathematical relationship of the stretching transformation of the FAST cable-nets when the working parabolic center is rotated in the direction of the $\overrightarrow{SC}$.

3.2. Geodesic tracing cable-nets node control algorithm

In the process of adjusting the ideal plane of the working state according to the radial telescopic constraint of the actuator, the geodesic tracing algorithm is used to select the region of the cable-nets. Based on the mesh division of the specular reflection structure of the cable network, the three-

dimensional ideal surface in space is realized through the geometric expansion of the plane shape. Then, the geodesic contour between any two points on the working surface [9] of the determined cable network was constructed and converted into the inverse mapping of the three-dimensional surface to solve the problem. The specific steps are as follows:

Step 1: Look for a strip of radiant triangular panel surface between any two given points, make sure that the line of the two points passes through all the triangular panels after the surface is geometrically projected on the plane, and then eliminate the extra triangles.

Step 2: According to the projection coordinates (D_1, D_2, D_3) of the three cable-net endpoints of the selected triangular panel on the plane, determine the center of gravity of the triangle:

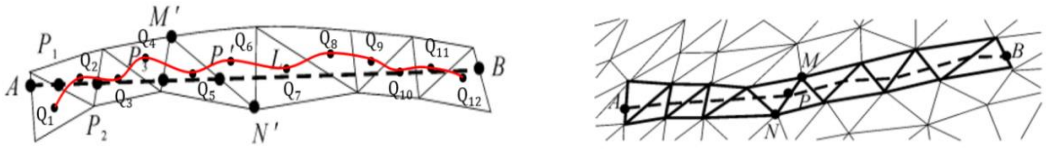
$$Q_i = \frac{D_i + D_{i+1} + D_{i+2}}{3}, \quad i = 1, 2, \cdots 3n \tag{6}$$

According to the knowledge of computer graphics [10], the coordinates of triangular cable-nets on the surface are expanded on the reference plane:

$$Q_i = R \times \begin{pmatrix} x_i \\ y_i \\ z_i \end{pmatrix} \times R^{-1} \left(R = \begin{bmatrix} \cos\gamma_i & \sin\gamma_i & 0 \\ -\sin\gamma_i & \cos\gamma_i & 0 \\ 0 & 0 & 1 \end{bmatrix} \cdot \begin{bmatrix} \cos\beta_i & 0 & -\sin\beta_i \\ 0 & 1 & 0 \\ \sin\beta_i & 0 & \cos\beta_i \end{bmatrix} \cdot \begin{bmatrix} 1 & 0 & 0 \\ 0 & \cos\alpha_i & \sin\alpha_i \\ 0 & -\sin\alpha_i & \cos\alpha_i \end{bmatrix} \right) \tag{7}$$

Assuming that there are n panels between the triangular strips of the surface, then perform n iterations to expand the spatial triangular panels into planar triangular strips until all triangular panels are projected onto the plane (As is shown in figure 5).

Step 3: Connect all the expanded panel triangle center of gravity, stretch and pull all the cables to give the geodesic.



(a) (b)

Figure 5. Reflection panel cables expansion (a) and mapping (b) schematic

Step 4: Taking the actuator telescopic constraint as the step size, the range of taking points is reduced step by step. Through computer simulation and search, determine the grid division of the active boundary contour of the geodesic line and the mirror panels layout schemes of the main cable structures supporting the FAST Reflectors.

Step5: The data of cable points in the A-E partition were calculated in sequence, and the inverse matrix was mapped to the working paraboloid to determine all the main cables in the grid of illuminated area to complete the geodesic tension control, and solve the expansion of each actuator.

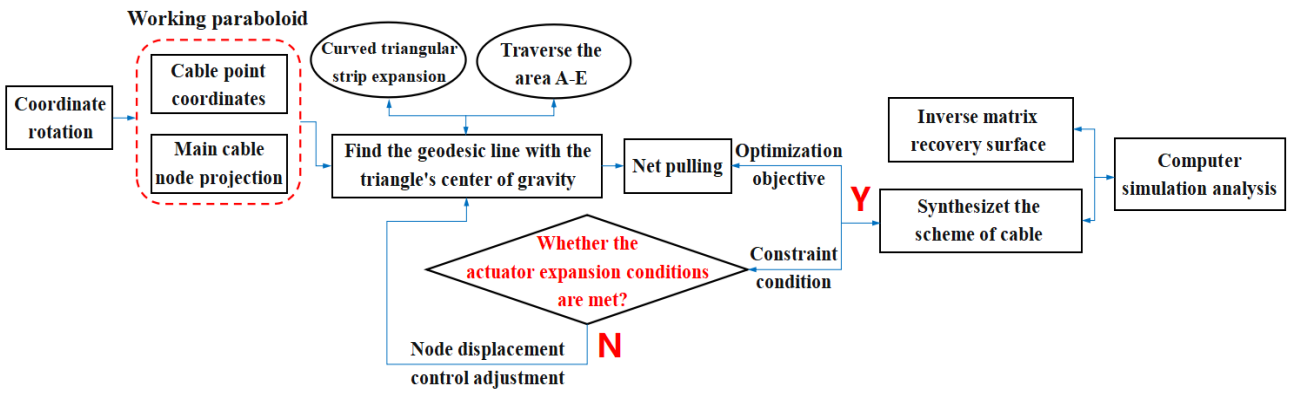


Figure 6. Flowchart of the geodesic tracing algorithm

The flowchart diagram of this algorithm is shown in Figure 6.

3.3. Actuators' telescopic constraint conditions

During the transposition process of the basic coordinate system at any angle, the radial expansion of the actuator is considered in combination with the adjustment factors of the reflector panel, so that it does not exceed the expansion scope.

Convert the original space rectangular coordinate system into a spherical coordinate system, the coordinate transformation equation is:

$$\begin{cases} x = \rho \sin\varphi \cos\theta \\ y = \rho \sin\varphi \sin\theta \\ z = \rho \cos\varphi \end{cases} \tag{8}$$

The polar equation of the radial actuation process of the cables of the working parabolic is:

$$\rho \cos\varphi = a^2 \rho \sin^2\varphi + h \tag{9}$$

Convert the equation to the maximum value of a quadratic equation in one variable describing the amount of actuating deformation:

$$\rho_{\max} = \frac{4a\sin^2\varphi h - \cos^2\varphi}{4a^2\sin^2\varphi}, \quad \varphi \in \left(\frac{\pi}{2}, \pi\right) \tag{10}$$

The steel cable points to radial actuation range constraint:

$$|\rho_{\max} - R| \leqslant 60cm \tag{11}$$

3.4. The solution results

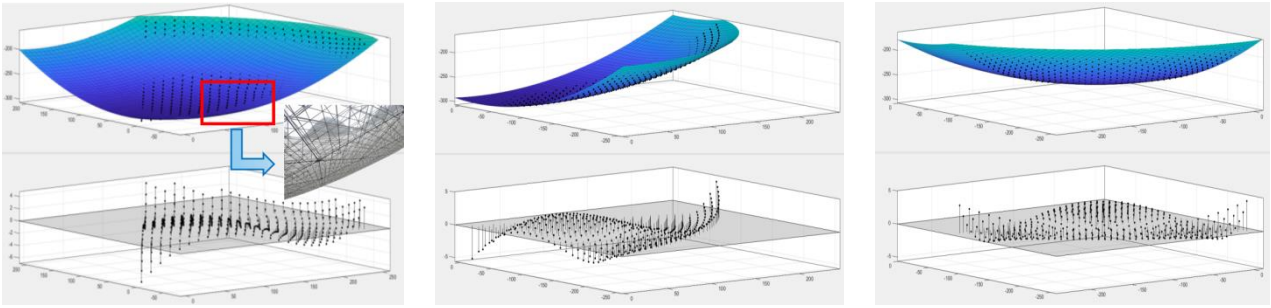
The total rotation matrix Λ_3 was applied to the main cable nodes in the coordinate system and converted into coordinates under the new coordinate system $C - x''y''z''$. According to the horizontal distance between the new coordinate system and axis Cz', find out all 692 points with horizontal distance within 150m and number them in sequence from near too far. Among them, the horizontal distance of the rotated coordinate of the D43 node was closest to the vertex under the paraboloid. Then through the returned rotation of the new coordinate system, the corresponding point coordinates in the initial coordinate system can be obtained.

By statistics, when $\alpha = 36.795°$, $\beta = 78.169°$, there are 743 main cable-net nodes in the illuminated area. Their telescopic amount all can be calculated by solving the geodesic solution and mapping relationships. Due to the large data, only the number and telescopic amount of part cable nodes at 30m caliber in the illuminated area with the new working paraboloid are shown in table 1.

Table.1. Expansion distance of partial main cable nodes (Unit: m)

Node	Expansion amount	Node	Expansion amount	Node	Expansion amount	Node	Expansion amount	Node	Expansion amount
D47	0.017716	E133	0.397461	E13	0.622192	C37	0.406641	E109	0.626850
D15	0.033815	C47	0.402520	D145	0.623440	D196	0.794299	A131	0.378003
D43	0.034864	C3	0.404278	C101	0.624047	B12	0.694380	D102	0.378959
D36	0.046460	C114	0.404689	D135	0.625523	C90	0.694382	E26	0.379215

As seen from table 1, within the cable network adjustment area of the given data, the number of cable network coordinate changes in area A and area B is significantly less than that in areas C, D, and E. In this case, figure 7(a) to figure 7(c) shows the analysis of the projection and cable-nets structures layout schemes of the FAST reflection panels in the zone of C-E:

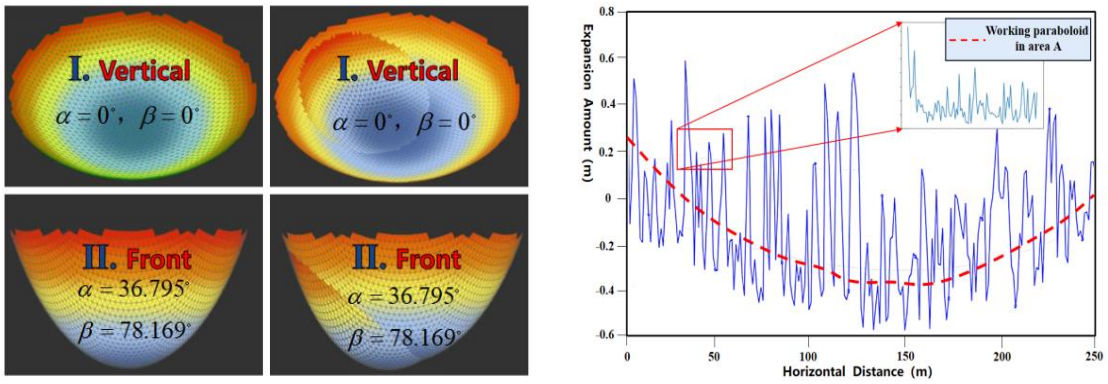


(a) (b) (c)

Figure 7. The stretch arrangement of reflective panel cable mesh about area C-E (from left to right)

Furthermore, because observed celestial body having a certain deviation from the original Cz axis, the overall working face will be inclined to the third quadrant of the overlooking plane. At the same time, it can be also found that the illumination area shifts to the lower left under the condition of this azimuth angle by adjusting the distribution law of each area's cable-nets.

Make the finite element analysis on the moving and stretching process of the cable network on the reference parabola of the working parabola of the reflection panel in the process of the cable network tension adjustment, and the data range of the cable network partition is given, and the relative motion position curve of the node profile is also made in figure 8(b).



(a) (b)

Figure 8. FAST cable-nets simulation analysis (a) and steel cable node actuation curve (b)

At this time, the working paraboloid equation in the rotating coordinate system is:

$$z = 0.001787835244(x^2 + y^2) - 380.0339141 \tag{12}$$

According to further analysis, the node with the minimum amount of expansion is numbered D47, and the minimum amount of expansion is 0.01776m, which is the main cable-nets node closest to the vertex coordinates of the new working paraboloid, with an adjustment of about 1mm. The nodes with the maximum amount of scaling are numbered D196 and the maximum amount of scaling is 0.794299m. The radial telescopic range of the actuators under each main cable node of FAST is $\pm$ 0.6m, and the telescopic range is 1.2m. The data results show that the expansion of the main cable nodes in this area is all within the scalable range.

4. Conclusions

In this paper, the model starts from the reflection mechanism of FAST information, and based on satisfying the physical law, adopts the analytic geometry method and the coordinate rotation transformation method to analyze the problem. The optimization and adjustment scheme of the main reflector of FAST is obtained by using the geodesic tracing algorithm. This algorithm can automatically deal with the topological changes of curves in the process of moving without any external control conditions. It is a fast algorithm suitable for computer implementation of the geodesic active contour models. By establishing the active model contour, optimizing the data structure, and applying the computer-aided simulation operation, the vertex coordinates of the ideal paraboloid and the control and the actuator adjustment of the FAST reflector cable net within the 300m aperture of the reflector can be well calculated. It has important guiding significance for radio astronomy and the morphological control of the cable of long-span steel structures.

Acknowledgements

The authors gratefully acknowledge Dr. Wang Xunyang for his technical support and financial support for further research in The National Mathematical Contest in Modeling for College Students.

References

[1] LI Tang.From KARST to FAST: The Conceptual Origin of FAST and Its Decision-making Process [J]. Acta Astronomica Sinica,2023,64(01):36-43.

[2] ZHU Zhongyi, ZHANG Lin, WANG Zhe, BAI Guangbo, LIU Chuanjia, LIU Fei, WANG Wei, LI Qingwei. Form-finding and structural behavior of cable net of Five-hundred-meter Aperture Spherical radio Telescope [J]. Journal of Building Structures,2021,42(01):18-29.

[3] Wang Yongrui, Liu Zhide. How to Setting out A Point in the Right-Hand Coordinate System with the Total Station [J]. Modern Surveying and Mapping, 2009,32(06):19+38.

[4] XING Xinkui, LEI Zhenlin, LI Qin, ZHU Wanxu. Study on the fatigue performance of FAST cable connecting structure [D]. Sichuan Building Science, 2018,44(03):34-38.

[5] Li Qing Wei, Jiang Peng, Li Hui. Prognostics and health management of FAST cable-net structure based on digital twin technology [J]. Research in Astronomy and Astrophysics,2020,20(5).

[6] LEI Huan, HUANG Yong-ning, HUANG Ying, SU Han. Study on Fatigue Performance of Main Cable in FAST Project [J]. Equipment Manufacturing Technology, 2016(11):1-5.

[7] CUI Yuxin, YANG Bin; YANG Yang, WANG Chaofei. Virtual Experiment Design of Euler's Rigid Body Rotation Theorem [J]. China Educational Technology & Equipment, 2021(08):28-30.

[8] Luo Shaohua, Liu Yang, Du Mingyi, Gao Siyan, Wang Pengfei, Liu Xiaoyu. The Influence of Spatial Grid Division on the Layout Analysis of Urban Functional Areas [J]. ISPRS International Journal of Geo-Information,2021,10(3).

[9] PIPELINES; Geodesic, environmental and archeological studies along route of Soyuz Vostok gas pipeline in Mongolia to begin in May [J]. Interfax: Russia & CIS Oil & Gas Weekly,2022.

[10] Michael N. Fried. Book Review: École polytechnique and descriptive geometry: STEM before STEM. Descriptive geometry, the spread of a polytechnic art: the legacy of Gaspard Monge [J]. Educational Studies in Mathematics,2020.